AWARD NUMBER: W81XWH-16-1-0045

TITLE: Discoidin Domain Receptors: Novel Targets in Breast Cancer Bone Metastasis

PRINCIPAL INVESTIGATOR: Dr. Hyeong-Reh Choi Kim

CONTRACTING ORGANIZATION: Wayne State University
5057 Woodward Ave.,
Detroit, MI 48202-4050

REPORT DATE: MAY 2020

TYPE OF REPORT: FINAL

PREPARED FOR: U.S. Army Medical Research and Materiel Command
Fort Detrick, Maryland 21702-5012

REPORT DOCUMENTATION PAGE

Form Approved
OMB No. 0704-0188

1. REPORT DATE	2. REPORT TYPE	3. DATES COVERED
MAY 2020	FINAL	1 Feb 2016 - 31 JAN 2020

4. TITLE AND SUBTITLE

Discoidin Domain Receptors: Novel Targets in Breast Cancer Bone Metastasis

5a. CONTRACT NUMBER
W81XWH-16-1-0045

5b. GRANT NUMBER
BC150621

5c. PROGRAM ELEMENT NUMBER

6. AUTHOR(S)

Dr. Rafael Fridman (Initiating PI)
Dr. Hyeong-Reh Kim (Partnering PI)

E-Mail: rfridman@med.wayne.edu and hrckim@med.wayne.edu

5d. PROJECT NUMBER

5e. TASK NUMBER

5f. WORK UNIT NUMBER

7. PERFORMING ORGANIZATION NAME(S) AND ADDRESS(ES)

Wayne State University
5057 Woodward Ave.,
Detroit, MI 48202-4050

8. PERFORMING ORGANIZATION REPORT NUMBER

9. SPONSORING / MONITORING AGENCY NAME(S) AND ADDRESS(ES)

U.S. Army Medical Research and Materiel Command
Fort Detrick, Maryland 21702-5012

10. SPONSOR/MONITOR'S ACRONYM(S)

11. SPONSOR/MONITOR'S REPORT NUMBER(S)

12. DISTRIBUTION / AVAILABILITY STATEMENT

Approved for Public Release; Distribution Unlimited

13. SUPPLEMENTARY NOTES

14. ABSTRACT Here we report major findings for our project aimed at studying the expression of Discoidin Domain Receptors (DDRs) in breast cancer (BrCa) tissues and their functional contribution to the formation of BrCa bone metastases. We also aim at testing the feasibility of targeting DDRs for the treatment BrCa bone metastases. During the current funding period, we identified pairs of BrCa samples from primary tumors and bone metastases. We performed studies to examine DDR1 expression. We found high levels of membranous DDR1 in both primary and metastatic cancer cells. MDA-MB-231 BrCa cells expressing wild type or kinase dead DDR1b were tested in a model of intraosseous tumor growth in female SCID mice. Histomorphometry analyses revealed that wild type DDR1b-expressing MDA-MB-231 cells displayed a tendency toward reduced intraosseous tumor burden when compared to control cells (no DDR1b expression). Interestingly, expression of the kinase dead DDR1b restore tumor growth when compared to cells expressing the wild type receptor. These results suggest that DDR1b may reduce the ability of MDA-MB-231 to grow within bone, and that this process requires kinase activity. We are conducting more analyses of the bone sections to confirm DDR1b expression and activation by immunohistochemistry. We are also conducting additional analyses to analyze bone response.

15. SUBJECT TERMS
Breast cancer, bone metastasis, discoidin domain receptors, kinases, targeted therapies, immunohistochemistry

16. SECURITY CLASSIFICATION OF:			17. LIMITATION OF ABSTRACT	18. NUMBER OF PAGES	19a. NAME OF RESPONSIBLE PERSON
a. REPORT	b. ABSTRACT	c. THIS PAGE			USAMRMC
U	U	U	UU	25	19b. TELEPHONE NUMBER *(include area code)*

Standard Form 298 (Rev. 8-98)
Prescribed by ANSI Std. Z39.18

Table of Contents

1. INTRODUCTION

Different treatments are currently used to treat bone metastasis, the main cause of morbidity and mortality in patients with advanced breast cancer (BrCa). However, although currently available therapies can be effective to relieve pain, prevent complications, and improve quality of life in these patients, are not curative. The identification of novel molecules involved in the establishment and expansion of BrCa metastatic cells within the bone is, therefore, crucial for the development of new prognostic biomarkers and therapeutic agents to prevent and/or inhibit skeletal metastases. Discoidin domain receptors (DDRs) are expressed in invasive BrCa and represent the only receptor tyrosine kinases (RTKs) that uniquely signal in response to collagen, a major organic component of the bone microenvironment. Based on these facts, the purpose of the research proposed in this application is to test our hypothesis that DDRs mediate the survival of metastatic BrCa cells within the skeletal niche and consequently represent promising targets for intervention in BrCa patients with bone metastasis. The scope of research involves the analysis of DDR expression in primary tumor and bone metastatic tissues from BrCa patients, the evaluation of therapeutic efficacy of DDR inhibition in a preclinical model of intraosseous BrCa growth, and the study of tumor-derived DDRs' role in the regulation of BrCa pro-osteolytic programs using *in vitro* systems.

2. KEYWORDS

Discoidin domain receptors, breast cancer, bone metastasis, receptor tyrosine kinases, collagen, biomarkers, targeted therapy.

3. ACCOMPLISHMENTS

- **What were the major goals of the project?**

Specific Aim 1. To conduct a histopathological analysis of DDR expression in samples of primary BrCa tissues with different subtypes and their matching bone metastasis.

Task 1: Select BrCa tissues for analyses and construct tissue microarrays (TMAs).

Task 2: Analyses of DDR expression.

Specific Aim 2. To evaluate the therapeutic efficacy of DDR inhibition in a preclinical xenograft model of intraosseous BrCa growth.

Task 1: Analyze DDR expression/activation and generate modified BrCa cell lines.

Task 2: Conduct animal studies to evaluate the role of DDRs in intraosseous tumor growth.

Specific Aim 3. To investigate the role of tumor-derived DDRs in regulation of BrCa pro-osteolytic programs in cell culture systems.

Task 1: Evaluate role of DDRs in regulation of pro-osteolytic factors.

Task 2: Conduct *in vitro* osteoclastogenesis studies.

- **What was accomplished under these goals?**

1) Major activities:

Specific Aim 1.

Aim 1, Task 1: Select BrCa tissues (primary and bone metastases) for immunohistochemical (IHC) analyses of DDR expression

We set to collect BrCa tissues for analyses of DDR expression. Our goal was to examine the expression in the primary site and the metastatic site (bone). To this end, we had to collect samples that included both primary and metastatic sites. Initially, we selected breast cancer tissues from the tissue bank at University of Michigan and generated a tissue microarray (TMA) containing triplicate samples of 120 invasive breast carcinomas including all breast cancer subtypes with comprehensive clinical and pathological information, including the presence of distant metastasis. Sixteen cases had presence of bone metastases. We subsequently devoted our efforts to identify additional primary invasive carcinomas and their corresponding distant metastasis from the same patients. This involved comprehensive searches in the surgical pathology databases form our institution and retrieval of blocks, some of which were stored in a different location. We encountered several problems, including the fact that in most cases, metastatic breast cancer to distant sites are minimally biopsied, which resulted in limited tissue available for immunostaining, the fact that several cases have been returned to other institutions, and because breast cancer metastasizes late (sometimes even 20 years) after primary tumor diagnosis, several primary tumors were over 15 years old. Despite these issues, we were successful in retrieving the cases described in detail in the tables below.

Aim 1, Task 2: Analyze DDR expression in the tissue samples.

Antibodies: To investigate DDR expression, we first focused on DDR1, a member of the DDR family of collagen receptors. To this end, we utilized a newly developed antibody (Ab) against human DDR1 that we obtained from Roche trough a Material Transfer Agreement with Wayne State University. This antibody binds the extracellular juxtamembrane region of all DDR1 isoforms and thus identifies receptor present on the cell surface. The antibody works under denaturing conditions and thus works well for immunohistochemical (IHC) analyses in paraffin embedded tissues. Consistently, the antibody does not work in immunoblotting. We tested the antibody in various IHC protocols and tissue samples known to express DDR1 or lack the receptor as well as in fixed cells that express or lack DDR1. These analyses confirmed its specificity for DDR1 and lack of reactivity with DDR2. We also worked out the optimal staining conditions for IHC.

Results: With this antibody in hand and an optimized protocol, Dr. Kleer conducted an IHC study with the breast cancer TMA, as proposed in task 2 of Aim 1. The staining was then evaluated by Dr. Kleer using the criteria of intensity of staining as 0 (negative), 1 (weak), 2 (moderate), 3 (strong); as well as the staining pattern (cytoplasmic, cell membrane, or both). DDR1 was

Table 1. Expression of DDR1

DDR1 Immunostaining	Cases	%
INTENSITY (n=120)		
No Staining	7	5.8
Weak	38	31.7
Moderate	59	49.2
Strong	16	13.3
SUBCELLULAR SITE (n=113)		
Cytoplasmic	54	47.8
Membranous	25	22.1
Both	34	30.1

localized in the tumor cells mostly in the cytoplasm (~48%) but also in the membrane (~22%).

Most of the samples (~49%) showed moderate staining for DDR1 (**Table 1**). No significant staining was detected in the tumor stroma. When the staining data was analyzed in relation to the histopathological features of the tissues, we found a lack of association between DDR1 expression levels and age, race, menopausal status, estrogen receptor (ER), progesterone receptor (PR), HER2-neu expression, tumor grade, tumor stage, or lymph node metastasis. Interestingly, however, we found a significant association between DDR1 protein localization and PR status, namely cytoplasmic DDR1 was significantly associated with negative PR expression (p=0.015) (**Table 2**). The biological significance of this finding is still unclear and thus remains to be determined.

Table 2. Association between DDR1 localization and categorical variables.

	Cytoplasmic		Membranous		C+M		
Variable	Cases	%	Cases	%	Cases	%	p-value
ER							0.40
Neg	19	38.0	8	32.0	7	23.3	
Pos	31	62.0	17	68.0	23	76.7	
PR							0.015
Neg	30	60.0	11	44.0	8	26.7	
Pos	20	40.0	14	56.0	22	73.3	
HER2							0.20
0	32	64.0	17	68.0	24	80.0	
1	9	18.0	3	12.0	1	3.3	
2	0	0	1	4.0	2	6.7	
3	9	18.0	4	16.0	3	10.0	
Menopause							0.36
Peri	6	12.2	1	4.0	4	13.8	
Post	36	73.5	17	68.0	17	58.6	
Pre	7	14.3	7	28.0	8	27.6	
Grade							0.88
1	6	11.8	1	4.0	3	10.7	
2	22	43.1	13	52.0	13	46.4	
3	23	45.1	11	44.0	12	42.9	
N Stage							0.96
0	22	52.4	10	47.6	16	55.2	
1	11	26.2	6	28.6	9	31.0	
2	7	16.7	3	14.3	3	10.3	
3	2	4.8	2	9.5	1	3.5	
Stage							0.87
1	15		9		11		
2	16		8		13		
3	11		6		4		
4	2		0		1		

Next, we conducted analyses to examine the relationship between DDR1 expression/ subcellular localization and patient survival. These preliminary analyses showed that cytoplasmic DDR1 was associated with shorter time to recurrence or death compared to C+M DDR1 (Hazard Ratio [HR] 2.03, 95% confidence interval [CI] 1.12-3.69, p=0.021). Interestingly, membranous DDR1 was associated with shorter time to recurrence or death compared to C+M DDR1 (HR 2.22, 95% CI 1.12-4.37, p=0.022) (**Fig. 1**).

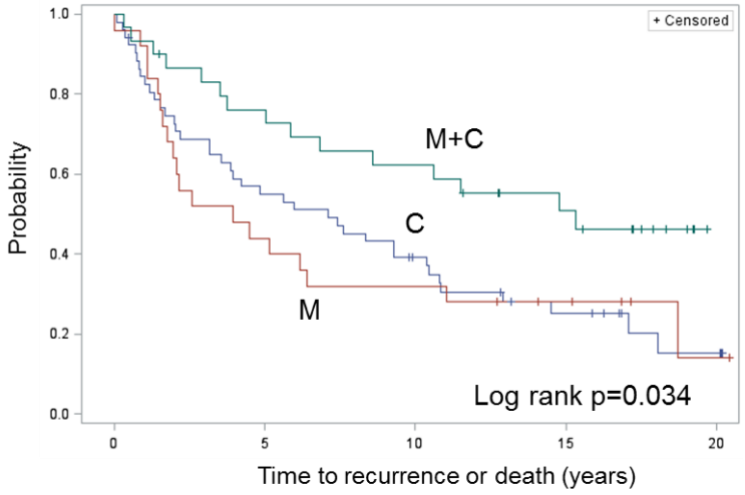

Figure 1. Kaplan Meier survival analyses showed that DDR1 localization is significantly associated with time to tumor recurrence or death.

Of the 120 cases of primary invasive carcinoma analyzed, 16 cases had presence of bone metastasis. Therefore, we wished to determine whether DDR1 expression in the primary tumor was associated with bone metastasis. However, this limited number of cases precluded achievement of statistical power and thus this issue remains unresolved.

Next, we identified, classified, and retrieved BrCa cases of primary and metastatic tumors from the University of Michigan surgical pathology files, which are described in **Tables 3 and 4**.

Table 3. Identified BrCa Samples.

Case	Type	Age at primary	Age at met	Histological type	Tumor Grade	Site of Bone Met
1	Metastasis	42	51	Lobular		paraspinal
	Primary			Lobular		
	Primary			Lobular		
2	Metastasis	61	72	Ductal		Bone
	Primary			Ductal	2	
3	Metastasis	72	77	Lobular		Left ileum
	Primary			Lobular	2	
	Primary			Lobular		
4	Metastasis	43	43	Ductal		Left iliac
	Primary			Ductal		
	Primary			Micropapillary	3	
5	Metastasis	62	62	Ductal		Left sacrum
	Primary			Ductal	2	
6	Metastasis	74	78	Ductal		R. ilium
	Primary			Mucinous	2	
7	Metastasis	41	67	Ductal	2	Left 5th rib
8	Metastasis	49	51			BM
9	Metastasis	49	73	Ductal		L. femoral head
10	Metastasis	58	60	Ductal		T9 vertebrae
	Primary			Ductal	3	
	Primary			Ductal		
11	Metastasis	42	44	Ductal		Lumbar vertebrae
	Primary			Ductal	3	
	Primary			Ductal	3	
	Primary			Ductal	3	
12	Metastasis	38	40	Ductal		R. femoral head
	Primary			Ductal	3	
13	Metastasis	49	49			L. distal humerous
	Primary			Ductal	1	
14	Metastasis	44	52	Lobular		Bone
	Primary			Lobular	1	
15	Metastasis	31	31			bone
	Primary			Ductal	3	
16	Metastasis	57	69			R. ilium
	Primary			Ductal	2	
17	Metastasis	49	61			R. Ilium
	Primary					
18	Metastasis	65	65	Lobular		R. Ileum
	Primary			Lobular	1	
19	Metastasis	65	65			T10
	Primary			Micropapillary	1	
20	Metastasis	73	73	Lobular		R. Ileum
	Primary			Lobular		

Table 3, Cont'd. Identified BrCa Samples.

Case	Type	Age at primary	Age at met	Histological type	Tumor Grade	Site of Bone Met
21	Metastasis	68	75	Lobular		L. iliac
	Primary			Lobular	2	
22	Metastasis	57	57			R. iliac
23	Metastasis	57	57			R. iliac
	Primary			Ductal and lobular	1	
24	Metastasis	69	69			T9
	Primary			Ductal and lobular		
	Primary			Micropapillary	3	
24	Metastasis	53	53			Left ilium
	Primary			Micropapillary	3	
26	Metastasis	35	57			T8
27	Metastasis	59	59			Left ilium
	Primary			Lobular	1	
28	Metastasis	63	63			bone
	Primary			Lobular	2	
29	Metastasis	34	37			left ischium
	Primary			Ductal and lobular	2	
	Primary					
30	Metastasis	41	50			Epidural/T-6
	Primary			Ductal	2	
	Primary			Ductal	2	
31	Metastasis	44	82	Ductal		sternum
32	Metastasis	54	54	Ductal		L5
	Primary			Ductal	3	
33	Metastasis	42	56			R. ilium
	Primary			Ductal	2	
34	Metastasis	44	73			R. ilium, L Sacrum
35	Metastasis	48	48	Lobular		bone
	Primary			Lobular	1	
36	Metastasis	57	62	ductal and lobular		T8/epidural
37	Metastasis	57	57	Lobular		L1
	Primary			Lobular	1	
38	Metastasis	49	52	Ductal		Femoral head
	Primary			Ductal	1	
39	Metastasis	77	78	Lobular		R. ileum
	Primary			Lobular	2	
40	Metastasis	38	39	Ductal		R. ileum
	Primary			Ductal	3	
42	Metastasis		66	Invasive papillary		Ischial

Table 4. Cases Selected for DDR1 Staining

	A	B	C	D	E	F	H	I	J	K	L	M	N	O	P	Q	R	S	T	U
1	Case	Cancer type	DDR1 expression M_membranous C_cytoplasm	Grade	Bone met	Type of specimen	ER	PR	HER2 status	Primary size	Lymph node mets	Other mets	Age of primary	Age of met	Survival	Last seen	Slides	Blocks	Number	Notes
2	SU-14-8532	Lobular	M negative_increased C and N		Left ileum	bx	pos	focally pos	neg			peritoneum	72	77	Deceased	9/19/15	Y	Y	A1	
3	BE-09-9872	Lobular	M negative_increased C	2		lump				4.3 cm	7 (0.8 cm)						Y	Y	2E-2F, 3B	
4																				
5	SU-15-41418	Ductal	M low		Left iliac	bx	pos (90%)	pos (90%)	equivocal (2+)			ovary	43	43	Alive-on c	Nov-17	Y	Y	A1	Scant
6	SU-15-38386	Ductal with micropapillary and lobular feat	M positive	3		mastectomy			Neg (by fish)	4.6 cm	16 (1.1cm)						Y	Y	A2, A13	
7																				
8	SU-15-72386	Ductal	M low_C increased		T9 vertebrae	bx	Pos (99%)	Neg (0%)	Neg (0+)				58	60	live	1-Nov	Y	Y	A1	
9	SU-14-15876	Ductal	M low_C increased	3		Lump	Pos (95%)	Pos (5%)	Neg (0+)	0.9 cm	38 (>2cm)						Y	Y	B4, A14	
10																				
11	SU-13-24588	Ductal	M low and negative areas _heterogeneous		R. femoral head	bx and res	pos (90%)	pos (20%)	pos (3+)			Possible lung	38	40	Went to C	2016	Y	Y	B2	
12	BE-11-28920	Ductal	M low	3		Lump	Pos	Pos	Neg (2+, fish n 2.6, 0.9, 0.2			2					Y	Y	1B, 1E, 7D, 9F	
13																				
14	SU-14-28105		M high		Epidural/T-6	res	pos (95%)	Few week 1.3%	Neg (1+)			Bone, liver, lung, a	41	50	Alive	1-Dec	Y	Y	A3	
15	BE-05-15918	Ductal	heterog_ M high and low_C increased	2		lump	Pos	Pos	neg	1.7 cm	2 (0.4cm)						Y	Y	1C, 1F-1G	
16																				
17	Su-14-29413		M high		R. Iliac	bx	Pos (80%0	Neg (0%)	Neg (1+)				57	57	Alive	Jun-17	Y	Y	A1	Scant
18	SU-14-30052	Ductal with lobular features	M high	1		bx	Pos (99%)	Neg (1%)	Equivocal (2+)								Y	Y	A1, B1	
19																				
20	SU-15-43142		M high		T9	bx						Melanoma and me	69	69	Alive	Apr-17	Y	Y	A1	
21	SU-15-50449	Ductal with lobular features	M high			bx	Pos (99%0	Neg (1%)	Neg (1+)								Y	Y	A1	
22																				
23	SU-14-30538		M low_C increased		Left ilium	Bx	Pos (90%)						59	59	Alive	Nov-17	Y	Y	A1	
24	SU-14-27290	Lobular	M low_C increased	1		bx	Pos (95%)	Pos (15%)	Neg (1+)	2.6 (imaging 1 (FNA)							Y	Y	A1	
25																				
26	SU-15-32662		negative		bone	BM bx	Pos	Neg	Neg			Bone, liver, peritor	63	63	Deceased	May-17	y	Y	A1	
27	BE-13-06193	Lobular	negative	2		bx	Pos (88%)	Pos (65%)	Neg (1+)								Y	Y	A1	scant
28																				
29	SU-14-71591	Lobular	M negative_C increased		L1	bx	Pos						57	57	Alive	Nov-17	Y	Y	A1	Super scar
30	SU-14-65607	Lobular ***NOTE LN DISSECTION***	M negative	1			Pos (98%)	Pos (79%)	Neg (1+)		12 (1.5 cm)						Y	Y	A2	
31																				
32	SU-14-1573	Lobular	M negative		R. Ileum	bx	Neg	Neg	Neg (0+)				38	39	Deceased	Mar-14	Y	Y	A1	Scant
33	BE-13-34846	Lobular	M negative	3		lump	Neg	Neg	Neg (1+)	3.2 cm		9					Y	Y	1I	
34																				
35	SU-13-33783	Lobular	M low_C increased		R. Ileum	bx	pos (90%)	neg (0%)	neg			Brain, liver, bone,	73	73	Deceased	Oct-14	Y	Y	A1	
36	SU-13-27858	Lobular	M low_C low			bx (chest wall)	Pos (30%)	neg (0%)	neg (1+)								Y	Y	A1	

From the cases depicted in Table 3, sections were cut from 12 matched primary breast cancers and their corresponding distant metastasis (**Table 4**). Of the 12 primary invasive carcinomas, 6 were Invasive Ductal Carcinomas (IDC) and 6 were Invasive Lobular Carcinomas (ILC). All metastases were to the bone. These specimens were processed for IHC analyses of DDR1 expression and subcellular localization. The IHC staining showed the following findings:

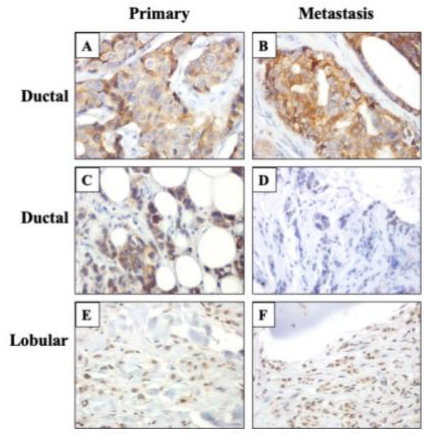

Figure 2. Representative images of DDR1 staining in BrCa samples of primary and metastatic tumors. **A**. Primary IDC with cytoplasmic and some membrane staining (BE-05-15918). **B**. Metastatic IDC with membrane expression (SU14 28105). **C**. IDC with DDR1 at the membrane (SU 15 38386). **D**. Metastasis, mainly negative, in cytoplasm (SU 15 41418). **E**. ILC with cytoplasmic DDR1 (no membrane) (SU 13 27858). F. Metastatic ILC with cytoplasmic DDR1 (no membrane) (SU 13 33783).

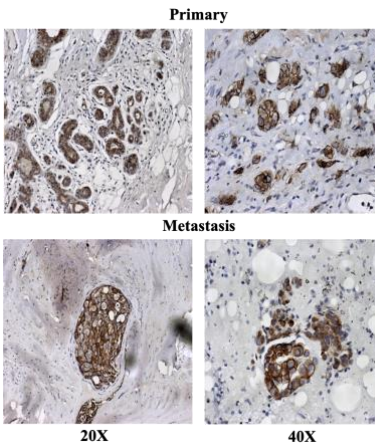

Figure 3. Representative images of DDR1 staining in BrCa samples of primary and metastatic tumors.

1. The primary and metastatic carcinoma have a similar expression level and pattern of DDR1 expression. Thus, in those samples, levels of DDR1 do not appear to be different between primary and metastatic tumors (**Fig. 2**).

2. Invasive ductal carcinomas (including ductal with lobular features) have frequent positive (or high) membrane expression in both the primary and the metastasis. This is consistent with DDR1 being a cell surface receptor (**Fig. 2A-D**).

3. Invasive lobular carcinomas tend to have low membrane, and increased cytoplasmic expression both in the primary and the metastasis (**Fig. 2E-F**).

4. The normal breast lobules around the invasive carcinoma and the DCIS are positive for DDR1 in the membrane (data not shown)

5. The pattern of expression in the primary tumors is similar to that of E-cadherin (membrane in ductal, reduced or cytoplasmic in lobular carcinomas).

In the last period (current 2019), Dr. Kleer identified additional pairs of primary and corresponding bone metastatic BrCa samples for IHC analyses. Although these analyses are still ongoing, we stained a few of the samples with the Ab against human DDR1 (**Fig. 3**). These analyses showed strong positivity in nest of tumor cells with DDR1 being mostly localized in the cell membrane, in both the primary and the metastatic tumors. At first sight, these IHC findings indicate that bone metastatic BrCa cells express high levels of DDR1. However, there is no apparent difference in DDR1 intensity of staining between BrCa cells in primary vs. metastatic site. Overall, the studies of Aim 1 are still ongoing and therefore a conclusion regarding the association between DDR1 expression and development of BrCa bone metastases cannot be established at this junction. Our collaboration with Dr. Kleer is still ongoing and we hope to address this association in the near future.

Specific Aim 2.

Aim 2, Task 1: Analyze DDR expression/activation and generate modified BrCa cell lines.

Our goal was to investigate the role of DDRs in intraosseous growth of breast cancer cells. Because breast cancer metastases is most frequently diagnosed in women with ER+ breast tumors, we proposed to use MCF7 cell line, which is ER+ and also can grow in bones of immunodeficient mice. Importantly, MCF7 cells express DDR1. Thus, these cells were utilized to examine the role of DDR1 in intraosseous tumor growth of ER+ breast tumor cells, as we proposed in the application. Women with triple-negative breast cancer (TNBCs) also can develop bone metastases. To test the role of DDRs in intraosseous growth of TNBCs we proposed to use MD-MB-231 cells (below). To this end, we purchased MCF7 and MDA-MB-231 cells labeled with luciferase from Cell Biolabs Inc. (San Diego, CA). We then examined expression of DDRs by immunoblotting using specific antibodies (**Fig. 4**). We compared the luciferase-overexpressing cells with control MCF7 and MDA-MB-231 cells. These analyses demonstrated that the MCF7-Luc cells express readily detectable DDR1, albeit at lower levels than the original MCF7 cells. MDA-MB-231-Luc cells showed no expression of DDR1 or DDR2, in our hands. In contrast, parental MDA-MB-231 cells showed low levels of DDR1 but not DDR2. Therefore, we decided to use the MCF7-Luc cells, which express and active DDR1 I response to collagen I, for our studies aimed at evaluating the contribution of DDR1 to intraosseous tumor growth, using a small molecule kinase inhibitor (described below) that targets DDR1.

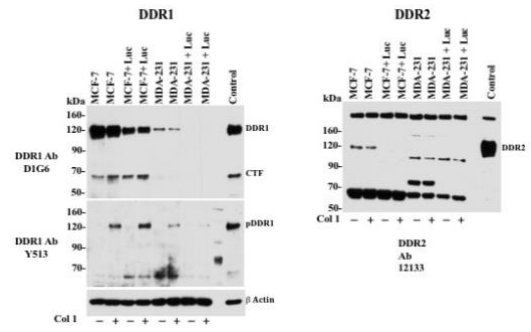

Figure 4. Expression of DDRs in MCF7 and MDA-MB-231 cells treated without or with collagen I. Cell lysates were processed for immunoblot analyses and examined for expression and activation of DDRs. The DDR1 Ab DIG6 recognizes total DDR1 whereas the Ab Y513 recognizes activated DDR1.

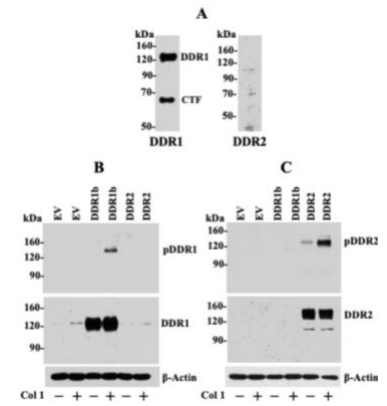

Figure 5. **A**. Expression of DDRs in parental MDA-MB-231 cells (Long exposure blots). **B and C**. Expression and collagen I-dependent activation of DDR1b (A) and DDR2 (B) in stable transfectants of MDA-MB-231 cells. Note that the blot in panel B is a short exposure and thus the endogenous DDR1 is not detectable. EV, control cells transfected with empty vector.

As we proposed, DDR1b (wild type and kinase dead) and DDR2 were ectopically expressed in MDA-MB-231 cells. The kinase dead (KD) DDR1b is a valuable construct to assess the biological effects of DDR1b that are mediated by its kinase activity. To this end, we generated stable transfects and collected pooled populations for analyses of receptor expression and activation. These analyses demonstrated that the pooled populations of stable transfectants expressed the corresponding recombinant proteins (only wild type DDR1 and DDR2 are shown). The wild type DDR1 and DDR2 were activated in response to collagen I, DDR1 ligand (**Fig. 5B-C**).

A New DDR1 Kinase Inhibitor: In the original application, we proposed to use a kinase inhibitor designated 7rj (J. Medical Chemistry 25; 3281-95, 2013). However, after the award of the application, we received a novel tyrosine kinase inhibitor (TKI) from Roche with excellent pharmacological and pharmacokinetics (pKa) characteristics. This proprietary inhibitor (referred to as Compound A here) exhibits high selectivity for DDR1 with an IC_{50} for DDR1 binding of 0.026 μM. In contrast, the IC_{50} for DDR2 binding is 2.3 μM, an 89-fold difference. Compound A also inhibits kinase activity of DDR1 with an IC_{50} of 0.018 μM. In kinase selectivity assays (468 targets), the DDR1 inhibitor preferentially targeted DDR1 with a K_d of 0.002 μM. In contrast, Compound A exhibited a K_d of 0.023 μM towards DDR2. When compared to the other targets, Compound A displayed >338-fold selectivity for DDR1. Roche also conducted pKa analyses in mice, which they have shared with us. We received this compound and tested it for inhibition of collagen I-induced activation of DDR1 and DDR2 in MCF7-Luc and BT549 cells, respectively. We reported that Compound A strongly and preferentially inhibited DDR1 collagen-induced activation but had no effect on DDR2 activation, under the same conditions.

Aim 2, Task 2: Conduct animal studies to examine the role of DDR1 in intraosseous growth of BrCa cells.

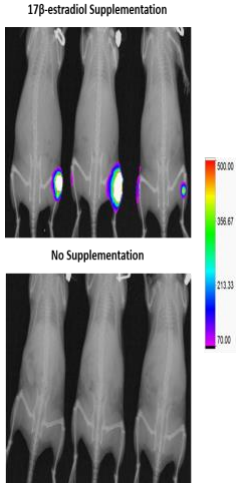

Figure 6. Representative whole-body bioluminescent and x-ray merged images of female nude mice supplemented with 17β-estradiol (top) or not (bottom) 4 weeks after intratibial injection with 10^5 MCF-7-Luc cells. The color scale indicates the intensity of photon emissions.

Animal Studies with the MCF7 Model. In the funding period we conducted multiple animal studies to investigate the role of DDR1 in intraosseous growth of BrCa cells. To this end, we utilized initially human BrCa MCF7-Luc cells. Mice were supplemented with estrogen to stimulate cell growth as MCF7 cells are estrogen receptor positive and require estrogen supplementation for growth. Because we purchased this cell line, it was important to test their ability to produce tumors when inoculated into the tibiae of immunodeficient mice. Briefly, $1x10^5$ MCF-7-Luc cells/mouse were inoculated into the tibiae of female nude mice. without estrogen supplementation or in mice which were implanted subcutaneously with 0.18 mg/90-day extended release 17β-estradiol pellets (Innovative Research of America, Sarasota, FL; Cat. # NE-121). We found that all mice receiving 17β-estradiol supplementation developed intraosseous tumors that were evident by bioluminescence (BLI) by week 4. In contrast, no signal was detected in the absence of 17β-estradiol supplementation, (**Fig. 6**). Thus, the MCF7-Luc system appeared to be appropriate to test the role of DDR1 in intraosseous tumor growth. We next tested the effect of the DDR1 inhibitor (Compound A) on MCF7-Luc cells implanted in the tibiae of immunodeficient mice. To this end, we developed the protocol depicted in **Figure 7**.

The protocol included two experimental groups of mice (n=9): Compound A- and vehicle-treated mice. Compound A was given daily, IP, at a dose of 90 mg/Kg as per Roche recommendation. Compound A was dissolved in 0.3% Tween-80, 0.9% NaCl. This solution was used as vehicle. Prior to tumor cell inoculation, 17β-estradiol 0.18 mg 90-day release pellets were implanted in the mice. A week later, mice were inoculated intratibially with $1X10^5$ cells per mouse. Treatment with Compound A or vehicle were initiated two days after tumor cell inoculation and administered daily, IP. Mice were subjected to bioluminescence imaging (BLI) every week, starting 5 days after treatment (=7 days after tumor injection), for a total of 4 times. To this end, mice were injected intraperitoneally with 150 mg/g D-luciferin in PBS, anesthetized with 2.5% isofluorane, and then imaged. **Figure 8** shows a representative BLI image of control and treated mice harboring MCF7-Luc cells, 4 weeks after tumor cell inoculation. For X-ray imaging, mice were imaged with a Bruker's In-Vivo Xtreme optical and x-ray small animal imaging system.

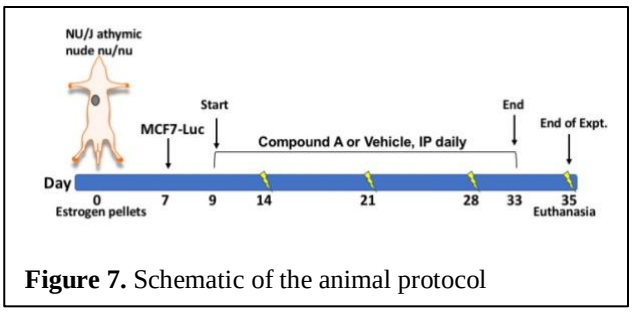

Figure 7. Schematic of the animal protocol

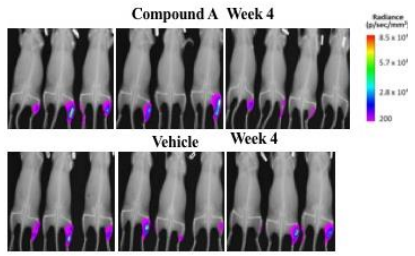

Figure 8. BLI of mice harboring MCF7-Luc tumors at 4 weeks.

For BLI quantitation of tumor growth, tumor sizes were calculated using the sum of total photon flux emission (photons/second/mm2) in the regions of interest (ROI) covering the entire tumors. ROIs from displayed images were quantified as total photon counts or photons/s using Living Image® software 4.0 (Caliper, Alameda, CA). The tumor growth rates across four-time points (Week 1 to 4) were compared using the linear mixed-effects model after tumor sizes were log-transformed. The model allowed for subject-specific baseline tumor size and tumor growth rate considering the correlation between time-dependent observations within the same subject. **Figure 9** shows the results of the quantitative analyses of BLI as a function of time. Disappointingly, these data showed no statistical significance between mice treated with Compound A and vehicle control. Next, we evaluated tumor size at the last time point (Week 4) (**Figure 10**). These analyses showed no statistical significance, indicating that there is no evident effect of Compound A on tumor burden in the

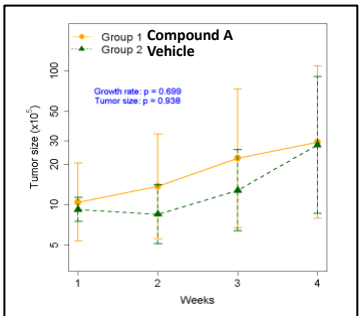

Figure 9. Time dependent quantitation of MCF7 intraosseous tumor burden by BLI in mice treated with Compound A or vehicle control. Tumor size at Week 4: Mean (95% CI). Compound A ($\times 10^5$ photons/second/mm2): 29.38 (7.91, 109.07); Vehicle ($\times 10^5$ photons/second/mm2): 28.05 (8.63, 91.19)

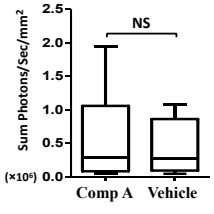

Figure 10. Quantitation and statistical analyses of MCF7 intraosseous tumor burden by BLI at week 4 in untreated and treated mice. Wilcoxon matched-pairs signed rank test

MCF-Luc model of intraosseous tumor growth. It is important to mention that there were no signs of toxicity in mice treated with Compound A, as determined by the weight and overall health of the mice.

Next, we conducted analyses of tumor burden by histomorphometry. To this end, ex-vivo tibia were fixed in 4% paraformaldehyde and imbedded in paraffin blocks. Paraffin sections (5 μm) derived from bone tumors were immunostained with Pan-cytokeratin (to identify epithelial cells) and counterstained with hematoxylin (H&E) (**Figure 11**). Digital photomicrographs of the entire histological section were captured at 5× magnification and stored as jpeg files. The entire image was then reconstructed using Adobe Photoshop. Tumor tissue (cytokeratin positive areas) and trabecular bone were isolated into separate layers and separately thresholded to black. The whole tissue cross sectional area (considered 100%) was then highlighted and the area occupied by either tumor or bone was automatically calculated. H&E stained bone sections revealed cluster of tumor cells growing with bone marrow cavities (**Figure 12**). Interestingly, examination of the sections also revealed abundant areas of dense bone tissue with reduced bone marrow spaces (**Fig. 12**, black arrow), suggestive of an osteoblastic response, possibly as a consequence of estrogen supplementation. Histomorphometry analyses of tumor burden, by measuring areas positive for cytokeratin, showed that these data agreed with the finding obtained by BLI, namely that there was no statistical difference in tumor burden between untreated and treated groups.

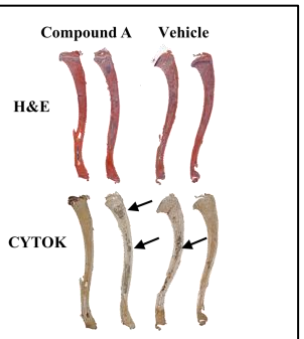

Figure 11. Representatives images of bones processed for H&E and pan-cytokeratin (CYTOK). Arrows show areas with tumor.

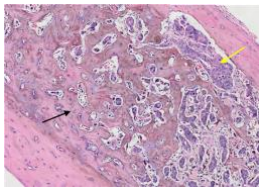

Figure 12. H&E of bone sections from tibiae of mice harboring MCF7-Luc tumors (yellow arrow). Black arrow shows the dense bone matrix present cells growing with bone. Upper panel 20X and lower

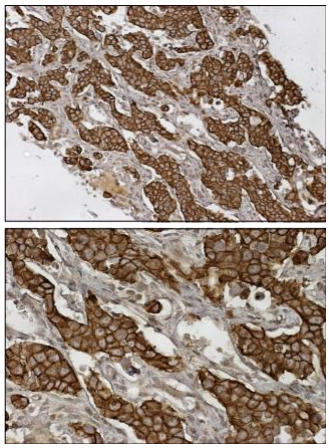

Figure 13. Expression of DDR1 in MCF7-Luc cells growing within bone. Upper panel 20X and lower panel 40X.

To verify that MCF7-Luc cells express DDR1 within the bone microenvironment, we performed IHC of bone tissue sections using antibodies that recognize only human DDR1. As shown in **Figure 13**, DDR1 is highly expressed in MCF7-Luc cells growing within bone, where it is mostly detected on the cell membrane, as expected. Thus, these analyses confirm that MCF7 cells express DDR1 in vivo, confirming the validity of the cell model for testing the contribution of DDR1 to BrCa intraosseous tumor growth. However, because DDR1 is a receptor tyrosine kinase that is phosphorylated in response to its ligand, it is also important to determine its phosphorylation status. At the time of this writing, this remains an unresolved issue and a technical challenge. We tested a commercially available antibody that recognizes phosphorylated DDR1b (at Y513), but the specificity of the staining was not convincing. We have recently identified another commercial source for a phosho-DDR1 antibody and we will be testing it soon. Therefore, at this junction, we cannot discern whether DDR1 is activated *in vivo*, and consequently whether Compound A is indeed targeting receptor activity (Discussed further in

Section 5, below).

Animal Studies with the MDA-MB-231 Model: We proposed to examine the roles of DDRs on intraosseous tumor growth utilizing another clinically relevant BrCa model, namely triple-negative BrCa cells. While most BrCa patients who develop bone metastases are estrogen positive, this site of tumor dissemination is also found in women with triple-negative tumors. To address this clinical situation, we also proposed to test the role of DDRs on intraosseous tumor growth of the triple-negative cell line MDA-MB-231. This cell line is known to grow within bone and to generate osteolytic tumors. In the context of our studies, we generated stable transfectants of MDA-MB-231 cells expressing wild type DDR1b or kinase dead DDR1b (a mutant with a K655A substitution within the kinase domain). These pooled cell populations were characterized for expression of the recombinant proteins and their ability to activate the recombinant DDR1b in response to collagen I stimulation. These analyses showed expression of the recombinant DDR1b receptors, as expected, and collagen I-mediated activation only of the wild type DDR1b, consistent with the K655A substitution inhibiting kinase activity (data not shown). With these cell lines in hand, the the last period of support (2018-2019) focused on conducting animal studies.

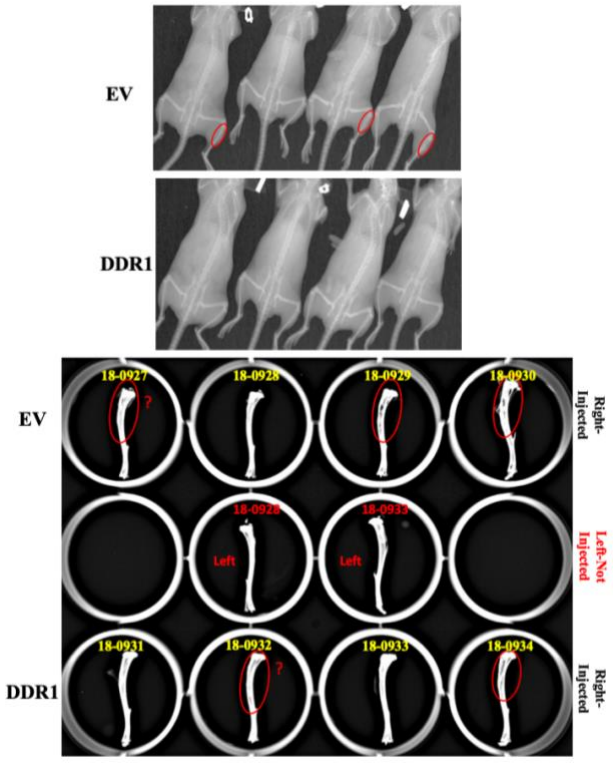

Figure 14. Upper picture: X-Ray imaging of whole mouse body after 4 weeks post-inoculation of MDA-EV and MDA-DDR1 cells. Lower picture: Ex-vivo X-Ray imaging of tibiae isolated from euthanized mice. Red circles show areas of osteolysis. Question marks indicate unclear response.

To confirm the ability of the MDA-MB-231 to grow within the bone, the cells were inoculated intratibially in female SCID mice. Specifically, we tested the ability of EV (empty vector) and DDR1b-expressing MDA-MB-231 cells to develop radiographically detected bone response upon inoculation into the tibiae of female SCID mice. Briefly, $2X10^5$ cells of MDA-EV and MDA-DDR1b cells were inoculated into the tibiae of mice (n=4 per group). After inoculation, the mice were imaged every week by X-ray using a Bruker's In-Vivo Xtreme optical and x-ray small animal imaging system. At 4 weeks post inoculation, based on the radiographic findings, the mice were euthanized. Tibiae were isolated and subjected to ex-vivo X-ray imaging.

As shown in **Figure 14**, X-ray imaging showed clear bone osteolysis in 3 out of 4 mice with cells inoculated with MDA-EV cells (upper picture). In contrast, mice inoculated with MDA-DDR1b cells showed no clear bone response (middle picture). When tibiae were imaged *ex-vivo* (lower picture), presence of osteolytic were readily seen in 2/4 mice inoculated with MDA-EV cells whereas one mice showed unclear response. The MDA-DDR1b bones showed 2/4 osteolytic regions. Based on these results, we concluded that the MDA-MB-231 transfectants are capable of growing within

the bone and produce radiographically detectable osteolytic lesions.

Given the ability of the MDA-MB-231 transfectants to grow within bone, we set to conduct an experiment with a larger number of mice as follow: MDA-EV (n=9), MDA-DDR1b WT (n=10), and MDA-DDR1b KD (n=10). In this experiment we also included the inactive KD of DDR1b. Mice were inoculated intratibially with $2X10^5$ cells. Mice were imaged every week by X-ray. Based on these data, mice were euthanized on week 3. The tibiae were isolated and processed for histomorphometry. For these analyses, *ex-vivo* tibiae were fixed in 4% paraformaldehyde and imbedded in paraffin blocks. Paraffin sections (5 μm) derived from bone tumors were immunostained with Pan-cytokeratin and counterstained with hematoxylin. **Figure 15** shows representative images of tibiae processed for histomorphometry. The images were analyzed to determine % tumor and bone areas in tibiae. The data obtained are depicted in **Table 5**. The data of Table 5 was plotted to determine the extent of intraosseous tumor growth, shown in **Figure 16**. These analyses revealed that upon expression of wild type DDR1b in MDA-MB-231 cells there was a tendency towards lower intraosseous tumor burden. However, unfortunately, this effect was not statistically significant. Interestingly, expression of the KD mutant of DDR1b abrogated the decrease observed with the wild type receptor. In fact, there was a statistically significant difference between the wild type and KD receptor. This suggests the hypothesis that DDR1b restricts intraosseous tumor growth of MDA-MB-231 in a kinase-dependent manner. There are a few analyses to complete these studies, including IHC analyses of DDR1 expression and activation, and TRAP staining.

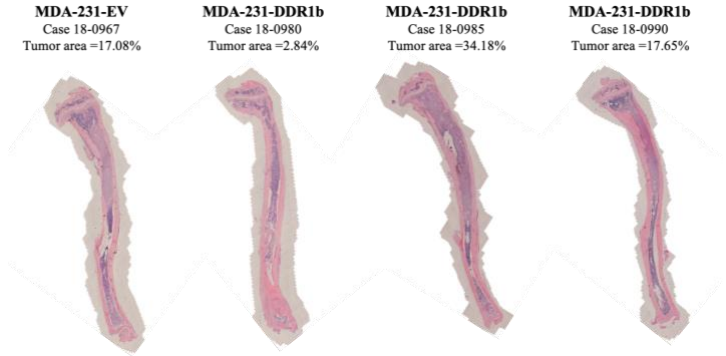

Figure 15. Representative images from H&E stained tibias harvested from mice inoculated with MDA-MB-231 variants, 3 weeks after tumor cell inoculation. Tumor areas were calculated, as described for Figure 11.

Table 5. Histomorphometry Analyses of Intratibial Tumors and Bone

Group	Mouse #	Tumor area (%)	Bone area (%)
MDA-231-EV	18-0965 T	3.39	23.96
	18-0966 T	14.44	60.55
	18-0967 T	17.08	38.44
	18-0968	0.26	32.77
	18-0969	-	49.26
	18-0970	0.77	50.36
	18-0971	0.23	39.29
	18-0972	0.52	53.24
	18-0973 (died)	NA	NA
	18-0974 T	11.14	44.86
MDA-231-DDR1b	18-0975 (died)	NA	NA
	18-0976	1.59	39.80
	18-0977 (died)	NA	NA
	18-0978	0.29	49.04
	18-0979	0.26	44.14
	18-0980 T	2.84	58.29
	18-0981	0.36	60.65
	18-0982	0.24	49.07
	18-0983	1.14	50.75
	18-0984	0.69	48.01
	18-0995	0.48	60.21
	18-0996	0.17	35.93
MDA-231-DDR1-KD	18-0985 T	34.18	41.21
	18-0986	0	51.88
	18-0987	0.41	52.96
	18-0988	0.34	48.36
	18-0989	0.07	57.42
	18-0990 T	17.65	51.37
	18-0991	0.41	46.65
	18-0992 T	12.31	46.85
	18-0993 T	3.98	55.15
	18-0994 T	4.95	50.13

T: evident tumor detected; NA, not applicable

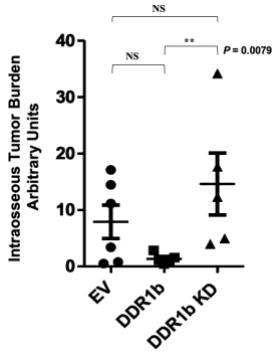

Figure 16. Effect of DDR1b (wild type and kinase dead) expression on intraosseous growth of human MDA-MB-231 cells in mice tibiae. EV, empty vector control; KD, kinase dead.

Specific Aim 3.

Task 1 and Task 2: Evaluate role of DDRs in regulation of pro-osteolytic factors. Conduct *in vitro* osteoclastogenesis studies.

Nothing to report. These studies were not conducted and are on hold. The reason for the delay is the fact that these analyses were contingent to the findings in the mice. Specifically, we hoped to determine whether the inhibition or overexpression of DDR1b would alter bone response, namely altering the ability of the BrCa cells to regulate osteolysis. In the case of the MCF7 cells, using Compound A, this could not be easily determined because the model system required estrogen administration, a potent inducer of bone formation. Under those conditions, any effects of MCF7 cells with or without Compound A administration were masked by the effects of estrogen. In the case of the MDA-MB-231 system, it is known that these cells induce a potent osteolytic response. Preliminary observation of the bone histology showed no striking differences in bone response. Also, the quantitative analyses of bone area showed no significant differences. However, we are currently conducting TRAP staining in the bone sections to determine whether there are alterations in the number of osteoclasts within bone. These results will provide more information on the potential role of tumor-associated DDR1b in regulation of the bone microenvironment.

2) Specific objectives:

The objectives during the period covered by this award were:

a. Use primary invasive breast carcinomas cases with matching bone metastases for analyses of DDR expression to establish whether there is an association between DDRs in the primary tumors and development of distant metastases.

b. Test the ability of a highly specific small molecule inhibitor of DDR1 in the ability of BrCa cell line to grow within bone.

c. Determine the role of DDRs in the MDA-MB-231 cell system of triple negative BrCa on intraosseous tumor growth.

d. Determine the role of tumor-derived DDRs in regulation of BrCa pro-osteolytic programs in cell culture systems.

3) Significant results or key outcomes:

Specific Aim 1, Tasks 1 and 2:

DDR1 is expressed in primary and bone metastatic lesions of IDC and ILC of BrCa. There is a differential subcellular localization of DDR1 in IDC vs. ILC tumors, with a more prominent membrane expression in IDC than in ILC. Strong DDR1 positivity in nest of tumor cells in both the primary and the metastatic tumors. Bone metastatic BrCa cells express high levels of DDR1. However, there is no apparent difference in DDR1 intensity of staining between BrCa cells in primary vs. metastatic site.

Specific Aim 2, Tasks 1 and 2:

A specific DDR1 kinase inhibitor, Compound A, had no apparent effect on the intraosseous growth of the estrogen positive human MCF7 cells.

Expression of wild type DDR1b in MDA-MB-231 restricts intraosseous growth when compared to KD DDR1b, suggesting that tis effect is kinase-dependent.

Specific Aim 3, Task 1 and Task 2:

No outcomes to report.

4) Other achievements:

Nothing to report.

- **What opportunities for training and professional development has the project provided?**

Nothing to report.

- **How were the results disseminated to communities of interest?**

Nothing to report.

- **What do you plan to do during the next reporting period to accomplish the goals?**

We are in a non-cost extension period. During the remining period we plan to do the following:

For Specific Aim 1, we will complete the analyses of the stained BrCa samples to determine association of histopathological features.

For Specific Aim 2, we will test the new antibody against pDDR1 to determine whether there are differences in receptor phosphorylation in the BrCa cells growing within bone. This will help to determine whether Compound A is effective in targeting DDR1 in the bone microenvironment.

For Specific Aim 3, we have no plans for these studies.

4. IMPACT

- **What was the impact on the development of the principal discipline(s) of the project?**

We hope to summarize all the data and report our major findings. In particular the IHC and animal studies. These findings will contribute to understand the role of DDR1 in BrCa bone metastases, in particular on the ability of tumor cells to survive within the bone microenvironment. We hope

also that our report will provide an insight into the challenges to analyze receptor function in vivo, in particular its phosphorylation status as a marker of inhibitor effect. Another impact may relate to the observation of a potential suppressive effect of DDR1 on tumor growth. This is unexpected as DDR1 is usually consider pro-oncogenic. This interesting possibility, however, needs further testing.

- **What was the impact on other disciplines?**

Nothing to report.

- **What was the impact on technology transfer?**

Nothing to report.

- **What was the impact on society beyond science and technology?**

Nothing to report.

5. CHANGES/PROBLEMS

As we reported last year, these inhibitor studies with the MCF7-Luc cells were unfortunately unsuccessful. We indicated that although the tibiae of mice inoculated with the MCF7-Luc cells developed intraosseous DDR1-positive tumors infiltrating into the bone marrow, the bones revealed significant areas of dense bone tissue with constricted bone marrow spaces. This effect, we speculated, possibly limited tumor expansion due to the generation of new bone in the presence of estrogen, a known inducer of bone formation. Importantly, treatment of mice with Compound A showed no evidence of anti-tumor effect when compared to untreated mice, as determined by quantitative imaging of tumors and histomorphometry. From these studies, we were unable to determine whether DDR1 plays a role in intraosseous tumor growth, under the experimental conditions used. The difficulty to determine whether DDR1 affected bone response also had a negative impact on the studies proposed for Specific Aim 3, which were not guided by the findings in the animal studies.

Actual or anticipated problems or delays and actions or plans to resolve them

We do not anticipate major problems for the remining of the non-cost extension period.

- **Changes that had a significant impact on expenditures**

Nothing to report.

- **Significant changes in use or care of human subjects, vertebrate animals, biohazards, and/or select agents**

Nothing to report.

- **Significant changes in use or care of human subjects**

Nothing to report.

- **Significant changes in use or care of vertebrate animals.**

Nothing to report.

- **Significant changes in use of biohazards and/or select agents**

Nothing to report.

6. PRODUCTS

- **Publications, conference papers, and presentations**

Nothing to report.

- **Website(s) or other Internet site(s)**

Nothing to report.

- **Technologies or techniques**

Nothing to report.

- **Inventions, patent applications, and/or licenses**

Nothing to report.

- **Other Products**

Nothing to report.

7. PARTICIPANTS & OTHER COLLABORATING ORGANIZATIONS

- **What individuals have worked on the project? See Note below Table**

Period: 1 Feb 2016 - 31 Jan 2017

Award W81XWH-16-1-0046: Dr. Fridman

Name	Project Role	Nearest Person Months Worked	Contribution to the Project	Funding Support
Rafael Fridman	Partnering PI	0.72	Design of experiments and data analyses	W81XWH-16-1-0046
Anjum Sohail	Research Scientist	4.2	Expression/activation analysis of BrCa cells, analysis of pro-osteolytic factors	W81XWH-16-1-0046

Award W81XWH-16-1-0045: Dr. Bonfil

Name	Project Role	Nearest Person Months Worked	Contribution to the Project	Funding Support
Ricardo Daniel Bonfil	Initiating PI	1.2	Design of experiments and data analyses	W81XWH-16-1-0045
Allen Saliganan	Research Assistant	6.6	Animal studies, immunohistochemical (IHC) assays	W81XWH-16-1-0045

Subcontract to Award W81XWH-16-1-0045: Dr. Kleer (Co-I, University of Michigan)

Name	Project Role	Nearest Person Months Worked	Contribution to the Project	Funding Support
Celina Kleer	Co-I	0.6	Evaluation and analysis of IHC	W81XWH-16-1-0045 (subcontract)
Maria E. Gonzalez	Research Associate	4.8	TMA construction, evaluation of IHC data	W81XWH-16-1-0045 (subcontract)

Period: 1 Feb 2017- 31 Jan 2018

Award W81XWH-16-1-0046: Dr. Fridman

Name	Project Role	Nearest Person Months Worked	Contribution to the Project	Funding Support
Rafael Fridman[2]	Initiating PI (9/17-present) Partnering PI (prior to 9/17)	0.72	Design of experiments and data analyses	W81XWH-16-1-0046
Anjum Sohail	Research Scientist	4.2	Expression/activation analysis of BrCa cells, analysis of pro-osteolytic factors	W81XWH-16-1-0046

Award W81XWH-16-1-0045: Dr. Bonfil/Kim

Name	Project Role	Nearest Person Months Worked	Contribution to the Project	Funding Support
Ricardo Daniel Bonfil[1]	Initiating PI (until 8/17)	1.2	Design of experiments and data analyses	W81XWH-16-1-0045
Hyeong-Reh Kim[3]	Partnering PI (9/17-present)	0.79	Design of experiments and data analyses	W81XWH-16-1-0045
Allen Saliganan	Research Assistant	6.6	Animal studies, IHC assays	W81XWH-16-1-0045

Subcontract to Award W81XWH-16-1-0045: Dr. Kleer (Co-I, University of Michigan)

Name	Project Role	Nearest Person Months Worked	Contribution to the Project	Funding Support
Celina Kleer	Co-I	0.6	Scoring and analyses of IHC data obtained for TMA and association with histopathological features	W81XWH-16-1-0045 (subcontract)
Maria E. Gonzalez	Research Associate	4.8	Selection of tissue blocks for processing, TMA construction, evaluation of IHC data	W81XWH-16-1-0045 (subcontract)

Note:
1. Dr. Bonfil, former Initiating PI, departed Wayne State University in August 2017. He is acting now as a Paid Consultant, as we reported at the time of his departure.
2. Dr. Fridman, former Partnering PI, became Initiating PI upon the departure of Dr. Bonfil.
3. Dr. Hyeong-Reh Kim became Partnering PI from September 2017.

Period 1 Feb 2018 – 31 Jan 2019

Award W81XWH-16-1-0046: Dr. Fridman

Name	Project Role	Nearest Person Months Worked	Contribution to the Project	Funding Support
Rafael Fridman	Initiating PI	0.72	Design of experiments and data analyses	W81XWH-16-1-0046
Allen Saliganan	Research Assistant	12	Animal studies, tissue processing immunohistochemistry	W81XWH-16-1-0046
Anjum Sohail	Research Scientist	3.0	Animal studies In vitro studies	W81XWH-16-1-0046
Benjamin Wasinski	Research Assistant	4.8	In vitro studies	W81XWH-16-1-0046

Award W81XWH-16-1-0045: Dr. Kim

Name	Project Role	Nearest Person Months Worked	Contribution to the Project	Funding Support
Hyeong-Reh Kim	Partnering PI	0.72	Design of experiments and data analyses	W81XWH-16-1-0045
Anjum Sohail	Research Scientist	1.8	In vitro studies	W81XWH-16-1-0045

Subcontract to Award W81XWH-16-1-0045: Dr. Kleer (Co-I, University of Michigan)

Celina Kleer	Co-I	0.6	Pathology analyses and tissue supplies	W81XWH-16-1-0045 (subcontract)
Maria E. Gonzalez	Research Associate	4.8	Processing of pathological tissues	W81XWH-16-1-0045 (subcontract)

Period 1 Feb 2019 – 31 Aug 2019[1]

Award W81XWH-16-1-0046: Dr. Fridman

Name	Project Role	Nearest Person Months Worked	Contribution to the Project	Funding Support
Rafael Fridman	Initiating PI	0.72	Design of experiments and data analyses	W81XWH-16-1-0046
Anjum Sohail	Research Scientist	3.0	Animal studies In vitro studies	W81XWH-16-1-0046
Benjamin Wasinski	Research Assistant	4.8	In vitro studies	W81XWH-16-1-0046

Award W81XWH-16-1-0045: Dr. Kim

Name	Project Role	Nearest Person Months Worked	Contribution to the Project	Funding Support
Hyeong-Reh Kim	Partnering PI (9/17-present)	0.72	Design of experiments and data analyses	W81XWH-16-1-0045
Anjum Sohail	Research Scientist	1.8	In vitro studies	W81XWH-16-1-0045

- **Has there been a change in the active other support of the PD/PI(s) or senior/key personnel since the last reporting period?**

Rafael Fridman, Initiating PI in this grant:

Nothing to report.

Dr. Hyeong-Reh Kim, Partnering PI

Nothing to report.

Celina Kleer, Co-Investigator in this grant:

Nothing to report.

- **What other organizations were involved as partners?**

Organization Name: Hoffmann-La Roche

Location of organization:	Basel, Switzerland
Partner's contribution to the project:	Supplied antibodies for DDR1 and a small molecule inhibitor for DDR1.

8. SPECIAL REPORTING REQUIREMENTS

Nothing to report.

9. APPENDICES

Nothing to report.